An Overview of Energetic Particle Measurements in the Jovian Magnetosphere with the EPAC Sensor on Ulysses

E. Keppler, J. B. Blake, M. Fränz, A. Korth, N. Krupp, J. J. Quenby, M. Witte, J. Woch

Observations of ions and electrons of probable Jovian origin upstream of Jupiter were observed after a corotating interplanetary particle event. During the passage of Ulysses through the Jovian bow shock, magnetopause, and outer magnetosphere, the fluxes of energetic particles were surprisingly low. During the passage through the "middle magnetosphere," corotating fluxes were observed within the current sheet near the jovimagnetic equato. During the outbound pass, fluxes were variably directed; in the later part of the flyby, they were probably related to high-latitude phenomena.

Ulysses, the fifth spacecraft to enter the Jovian magnetosphere, found it in very extended state compared to previous observations. The measurements revealed its highly dynamic nature and confirmed that Jupiter is an important source of energetic particles in interplanetary space. Ulysses found in the magnetosphere particles of solar origin, others originating in the Jovian atmosphere, oxygen and sulfur released from Io, and ions possibly sputtered from other moons. The variety of particle sources provides clues on acceleration mechanisms within the Jovian magnetosphere. For the first time, fluxes of charged particles have been measured in three dimensions, which provided new insight into the topology of the magnetodisk and the distribution of charged particle fluxes.

Energetic Particle Composition Instrument (EPAC) consists of four essentially identical three-element silicon semiconductor surface-barrier telescopes with a field of view of 36°. The central axes of the telescopes form angles of 22.5°, 67.5°, 112.5°, and 157.5° with respect to the spacecraft spin axis (Fig. 1). The detectors have thicknesses of 5, 100, and 300 μm from front to back. The first two detectors are used to determine (i) the particle identity from its energy loss and (ii) the total energy of incident particles. The third detector serves as a veto. The instrument measures protons in the energy range $0.3 < E < 1.5$ MeV, heavier ions in the energy-nucleon range $0.4 < (E/\text{nuc}) < 6$ MeV, and electrons in two energy channels ($0.1 < E < 0.4$ MeV and $E > 0.18$ MeV). The geometrical factor of the telescopes is 0.08 cm^2 sr (*1*).

During approach to Jupiter (Fig. 1) in early January 1992, Ulysses encountered a corotating interplanetary particle event with fluxes of protons and heavier ions up to two orders of magnitude above background. The event ended by 22 January, when Ulysses was about 300 Jovian radii (R_J) from Jupiter and to the west of the Jupiter-sun line (Fig. 2).

In the early part of the event (day 6) the proton fluxes exhibited rather large anisotropies (*A*) peaked in the solar direction, up to $A = 0.9$, which later decreased to $A = 0.5$ for the remainder of the period. The exponent for differential power-law energy spectra during this period, varied around 1.4 for protons and 2 for helium ions. The spectral variability resulted in a remarkable variability in the relative abundances as a function of energy (taken at equal velocities). The values of the p/He ratio ranged from 27 at 400 keV/nuc to 50 at 1 MeV/nuc. Electrons above 180 keV show a persistent anisotropy of 0.6 (not shown), peaked in the direction of Jupiter. The lower energy channel was at background through this period. On day 8, ~100-keV ($100 < E < 400$ keV) electrons from the solar direction were superposed on the continuing anti-solar flow >180-keV electrons (Fig. 2). Although these fluxes were nearly isotropic over most of the time Ulysses was upstream of Jupiter, anisotropies of the order 50% were observed during day 29; moreover, very large anisotropic fluxes (up to 99%) were observed along the Parker spiral angle (angle of the average interplanetary magnetic field vector with the radius vector) after day 30, in particular during the event centered at 00:00 UT (universal time) on day 32 (Fig. 2).

Closer to the Jovian magnetosphere (after day 31, Fig. 2) particle fluxes increased steadily and became fully isotropic when the Jovian bow shock was reached. In general, after 31 January, when Ulysses was at about 160 R_J from Jupiter and 54 R_J from the magnetopause (as observed later), particle fluxes (protons, electrons, and heavier ions) increased almost monotonically with diminishing distance from the planet. Also at that time >100-keV electrons reappeared, predominantly from the solar direction; the spectral index for electrons increased to values >5. Two superposed small increases in ion fluxe were observed. This event is interpreted as similar to events observed upstream of Earth's bow shock. Most remarkable, however, the p/He ratio taken at 1 MeV/nuc fell to about 10 just in front of the magnetopause. This change was a consequence of the rapid softening of the proton spectrum as Ulysses approached the magnetopause. For a power law in energy per nucleon, the spectral index increased from 2.3 at 134 R_J to 4.7 at 100 R_J, whereas the spectral index for helium did not change significantly during the same time period.

The Jovian bow shock was passed at 17:33 UT on day 33 (*2*), and at about 2 R_J farther inward the Jovian magnetopause was reached (at 21:30 UT). The latter event is clearly seen in the electron data (Fig. 3). About 1 R_J upstream of the magnetopause the spectral index increased steadily from 1.7 to 2.8 (power law exponent), which was reached at the magnetopause. Electron fluxes became isotropic near the bow-shock crossing without a significant change in intensity. Twenty minutes after Ulysses passed through the bow shock, protons with energies $E > 300$ keV increased by a factor of 6 for about 1 hour mainly from the solar direction ($A > 0$) and then diminished by a factor of 2 between the bow shock and the magnetopause. Also, the helium flux decreased by a factor

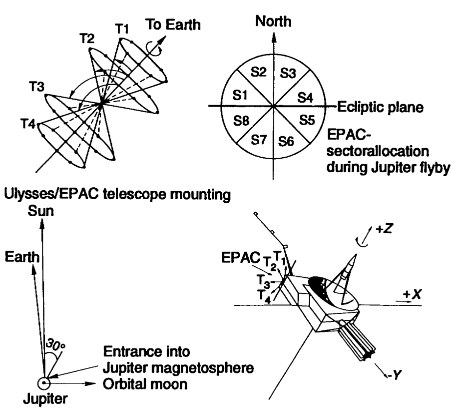

Fig. 1. Viewing directions and relative position of the four telescopes in the spacecraft. Sectors S1, S2, . . . ,S8 (same for all four telescopes) are covered subsequently in that order. View is toward Earth, that is, S1 is pointing to the east, S4 to the west. The geometry of the Jupiter encounter is illustrated in the lower left.

E. Keppler, M. Fränz, A. Korth, N. Krupp, M. Witte, Max-Planck-Institut für Aeronomie, D-3411 Katlenburg-Lindau, Germany.
J. B. Blake, Aerospace Corporation, Space Science Laboratory, Los Angeles, CA 90009.
J. J. Quenby, Imperial College of Science and Technology, Blackett Laboratory, London, United Kingdom.
J. Woch, Swedish Institute of Space Physics, Kiruna, Sweden.

of 5 to 3 particle cm^{-2} s^{-1} sr^{-1} during this period. Further crossings of the magnetopause, as reported in (3), are barely visible in our electron data (Fig. 3).

When Ulysses passed through the magnetopause, the ~100-keV electron intensity increased suddenly by a factor of 50. At the same time the higher energy electron flux jumped by almost a factor of 1000. Throughout the region, which extended from the magnetopause crossing at 106 R_J to a boundary located near 82 R_J, the ion fluxes remained at about the level that was observed just inside the magnetopause. In contrast to the ion flux, the electron flux showed variations in intensity although the well-known 10-hour periodicity (the planet's rotation period) was clearly evident only in the spectral slope, illustrated by the ratio of the two electron channels (Fig. 3). Higher values (2.7) were reached when Ulysses was in the current sheet. Outside of the sheet the spectral index decreased to 1.9, predominantly higher energy electrons were present because of their larger gyroradii, and low-energy electron fluxes increased toward the sheet. The ~10-hour periodicity became out of phase somehow, when in the middle magnetosphere such periodic intensity variations were also seen in the ion fluxes.

No remarkable effects were seen in the ion flux while Ulysses passed through the outer magnetosphere; fluxes were low (of the order of a few particles per square centimeter per second per sterodian). After Ulysses passed through the boundary mentioned above and entered the "middle magnetosphere" on day 35, 10:50 UT, however, the energetic particle environment changed dramatically.

Electrons, protons, helium, oxygen, and sulfur fluxes increased by more than an order of magnitude, and the ion fluxes varied in intensity with magnetic latitude; this result is evident in the periodic encounter of the spacecraft with the equatorial current sheet. The first flux maximum (Fig. 3, curve 5) was at a magnetic latitude of ~4°S (2), the second to fourth maxima were at smaller and smaller south latitudes, and the fifth maximum was near the nominal magnetic equator.

In contrast, the first flux minimum (indicated by a number with a star) was observed at about 26°N, the fifth at about 20°N. The ion flux maxima became marginally smaller, whereas the flux minima decreased systematically as Ulysses moved farther inward. These differences were probably due to differences in the position of Ulysses with respect to the current sheet. The observations are consistent with a model of the current sheet (4, 5), in which the plasma sheet, nominally normal to the magnetic axis of Jupiter, becomes inclined by centrifugal forces out of the dipole line of zero latitude and toward the equatorial plane defined by the rotational axis. The

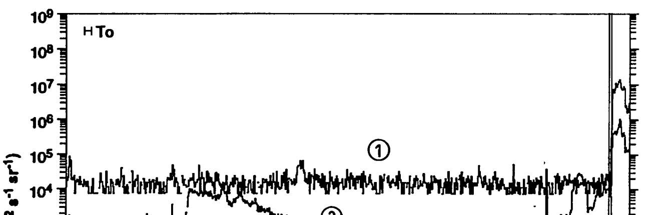

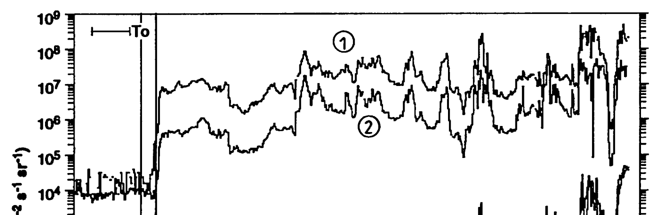

Fig. 2 (left). The period from 1 January through 4 February 1992 (day of year 1 through 35) before Ulysses reached the Jovian magnetosphere, BS, bow shock; MP, magnetopause (3), Io, Jupiter rotation period. The various curves, identified by encircled numbers, are as follows (1-hour averages): 1, electron fluxes $E > 0.18$ MeV ($\times 10^4$); 2, electron fluxes 0.1 $E \leq 0.4$ MeV ($\times 10^3$); 3, proton flux $E > 300$ keV, spin averaged, telescope 2; 4, proton flux $E > 500$ keV, spin averaged, telescope 2; 5, helium flux, E/nuc > 400 keV/nuc, omnidirectional (summed over all telescopes, spin averaged); 6, oxygen flux, E/nuc > 400 keV/nuc, omnidirectional (summed over all telescopes, spin averaged); 7, flux ratio of sulfur to oxygen, E/nuc > 400 keV/nuc; 8, flux ratio of oxygen to helium, $E > 400$ keV/nuc; 9, flux ratio of protons to helium, E/nuc > 400 keV/nuc; 10, spectral slope of electron spectra; and 11, anisotropy of proton fluxes (telescope 1 − telescope 4)/(telescope 1 + telescope 4). **Fig. 3 (right).** Same as in Fig. 2, but for the inbound pass through the Jupiter magnetosphere during 2 to 8 February 1992. Numbers in the upper part under curve 6 refer to maxima and minima of ion fluxes, mentioned in the text.

first passages of the spacecraft into the current sheet are extended through the center of the sheet (2) and thus show two maxima separated by a relative minimum in intensity (Fig. 3). Typical pitch-angle distributions obtained during this period are displayed in Fig. 4A for ~0.6-MeV protons during the fourth flux maximum and the subsequent minimum. A sample of the flux distribution in three dimensions, taken at 17:00 UT (5 February), is shown in Fig. 4B. Fluxes tend to peak around a pitch angle of 90° during flux maxima (inside of the current sheet), but Fig. 4B also shows the fluxes impinging from the corotation direction are due to a population of protons, the center of gyration of which lies about 1 R_J south of the position of Ulysses. This is consistent with positively charged particles gyrating in an outwardly directed planetary magnetic field at a pitch angle of 90°. Fluxes are peaked at 0° or 180° pitch angle during flux minima (outside the current sheet), indicating particles streaming away from the planet. The frequent jumps between 0° and 180° pitch angle seem to be correlated with the current sheets discussed in (3).

This regime breaks down on day 37, when the 10-hour periodicity became out of phase but did not disappear. The flux maxima inside of the current sheet increased, as did the flux minima outside of the current sheet. On day 38 all fluxes disappeared for about 2 hours and afterward the fluxes of all species rose dramatically; these effects are probably related to entry of Ulysses into the dipole fieldline regime of the inner magnetosphere (Fig. 5). The flux minimum that was observed between 20 and 22 UT on day 38, when the spacecraft was at high magnetic latitudes, may indicate that Ulysses encountered the Jovian equivalent of the cusp region; the counting rates of all of our detectors were at the interplanetary background level. After the next flux increase the EPAC instrument was turned off for safety. It was turned back on after closest approach on 02:50 UT, day 40.

During day 39, Ulysses remained at relative low magnetic latitudes and continued to move in and out of the current sheet, as indicated by the flux variations in all species. This situation continued until day 40, when Ulysses reached 25°S. The onset of a new regime was particularly visible in the electron data (Fig. 6). Proton fluxes varied significantly during this first phase: the energy spectra steepened during the flux maxima and flattened during minima. Also, the relative abundances of ions changed: in the flux maxima, oxygen and sulfur increased relative to helium whereas proton abundances decreased relative to that of helium.

The electron spectrum became continu-

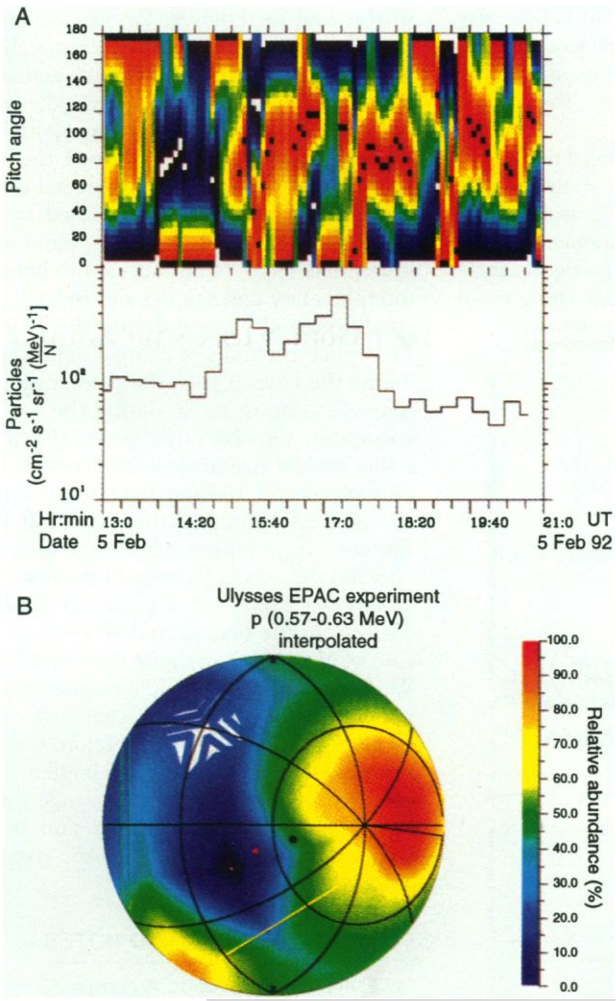

Fig. 4. (**A**) (Lower panel) Differential flux of protons (0.57 ≤ E ≤ 0.63 MeV) summed over all telescopes and averaged over all sectors. (Upper panel) Relative differential flux variations (color code) versus pitch angle and time. Black dots give pitch angle of flux maxima, white dots for the minima. Pitch angle 0° means particles are moving parallel to the magnetic field. (**B**) Relative differential fluxes (color code 0 to 100%) shown on a sphere, the spacecraft is in its center, spin axis is horizontal and Earth-pointing, north is upward. Jupiter's position is given by a black circle, the magnetic field direction by a red triangle. (White areas in upper left are artifacts.) Measurement has been taken at 17:00 UT on 5 February; sampling time was 4 min.

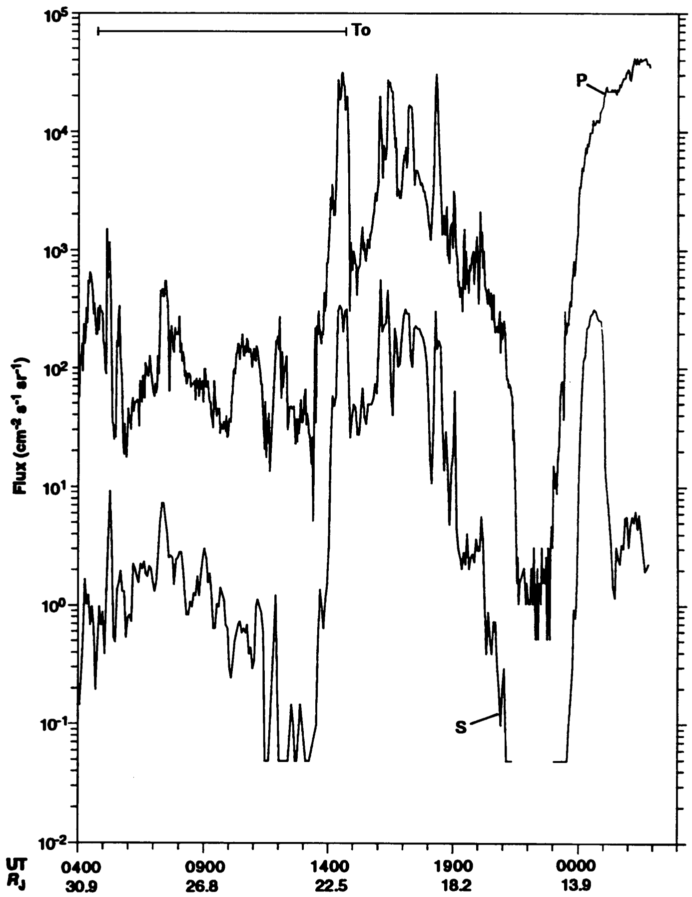

Fig. 5. Fluxes of sulfur (S) and protons (P) (E/nuc > 400 keV/nuc) for the innermost part of the inbound pass, 7 February 1992, 4:00 UT, to 8 February 1992, 4:00 UT, just before instrument turn-off.

Table 1. Ion composition [relative composition, normalized to oxygen (≡1)] inside ("in," during flux maxima) and outside ("out," during flux minima) of the current sheet.

Time	H	He	C	N	O	Ne	Na	Mg	Si	S	Fe
In	360	18	0.08	0.09	1.0	0.04	0.035	0.03	0.045	1.5	0.25
Out	760	38	0.15	0.075	1.0	0.036	0.06	0.07	0.05	1.2	0.3

ally flatter during the outbound pass; after day 41 Ulysses remained above 25°S. The structure of the flux variations became more irregular, the p/He ratio remained more or less constant, while the flux of heavier ions (oxygen and sulfur) decreased much more than that of the lighter ions, presumably the result of the different origin of protons and helium compared to oxygen and sulfur. There were several such situations, where these two elemental groups showed different behavior (see Figs. 2 and 3). The sulfur/oxygen ratio during the outbound pass resembled that measured in the outer magnetosphere on the inbound pass. During the outbound pass the anisotropy *A* of protons shows burst-like variations (Fig. 6, curve 11) (*A* up to +0.7). A positive value of *A* means that more protons are observed in telescope 1 than in telescope 4. As long as the spacecraft was inside the Jovian magnetosphere (until 14:00 UT on 12 February 1992) telescope 1 looked approximately into the direction of the magnetic field (not shown). This means that a positive anisotropy corresponds to proton fluxes antiparallel to the magnetic field direction.

The magnetopause was crossed for the first time outbound on 13:57 UT, day 43 (*1*). Subsequently, the magnetopause was crossed several times. The crossings were indicated in the particle data by large decreases in all fluxes. Only during the last crossing from 9:10 until 21:40 UT on day 45 did the flux even for the Iogenic ions (oxygen and sulfur) increase greatly. After that, Ulysses completely left the Jovian magnetosphere at 124 R_J.

The ion composition changed inside and outside the current sheet, as shown by the elemental ratios (Figs. 2, 3, and 6, and Table 1). The relative abundance of the heavier ions did not change significantly between the two regimes, but the ions of lower masses (helium, carbon, nitrogen) became more abundant outside of the current sheet. This difference could be due to the easier access of solar particles to these regions as compared to the current sheet region. The increase in the relative abundance of sodium and magnesium in the region outside of the current sheet could be due to ion sputtering from the surfaces of the outer moons of Jupiter.

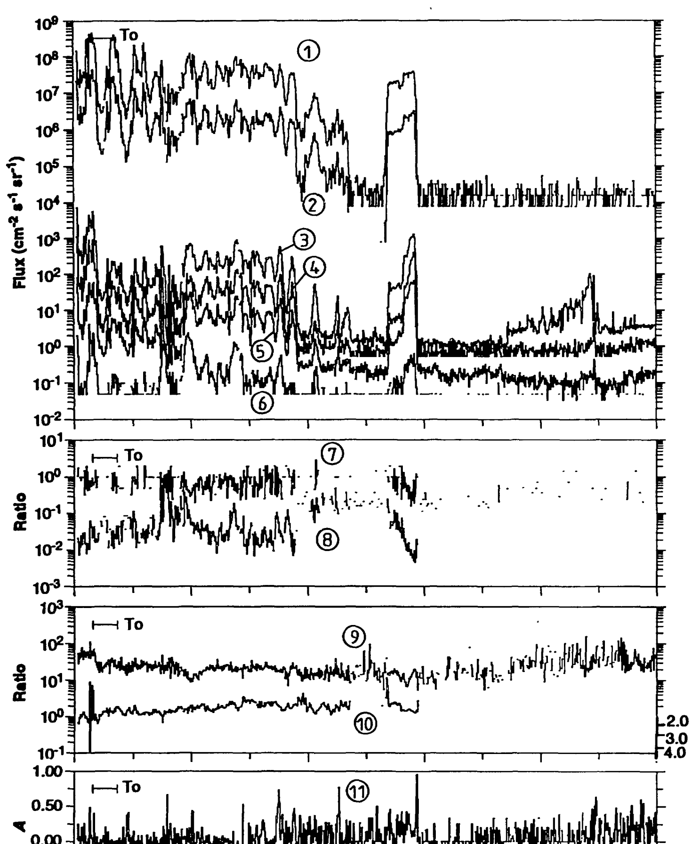

Fig. 6. Same as in Fig. 2, but for the outbound pass through the Jupiter magnetosphere during 9 to 19 February 1992.

Because of orbital constraints, spacecraft have entered the Jovian magnetosphere near the 10–local time meridian. Pioneer 11 (*6*) in particular followed a path similar to that of Ulysses; except for exchange of the in- and outbound portions in magnetic coordinates; the orbits of both satellites were almost the same. Therefore, a closer comparison of data obtained with Ulysses and Pioneer 11 seems to be warranted. As in the case for Ulysses, Pioneer 11 on its unbound trajectory passed through a boundary at about 65 R_J, which terminated a region that we called the "middle magnetosphere" (*6*). Unlike Ulysses, on the inbound pass Pioneer 11 crossed the bow shock and the magnetopause several times, all of which might have occurred in the outer magnetosphere. Thus, the outer magnetosphere seems to be affected by changing interplanetary conditions, and indeed such conditions did change during the Pioneer 11 passage but did not change significantly during the Ulysses pass: the outer magnetosphere was more stable during the Ulysses encounter. On the other hand, this more stable middle magnetosphere regime, with its pronounced 10-hour periodicity caused by repeated entries of the spacecraft into the corotating magnetodisk, is visible not only in Ulysses and Pioneer 11 data but also in Voyager 2 data (*7*) at a distance of about 65 R_J from the planet, and at 49 R_J in the case of Voyager 1 (*8*) and Pioneer 10 (*9*). We believe that this middle magnetosphere is only weakly affected by changing interplanetary conditions and therefore was encountered in all missions to Jupiter. It is characterized by the current sheet with large fluxes of heavy particles and by its composition of protons, helium, oxygen, and sulfur ions.

REFERENCES AND NOTES

1. E. Keppler *et al.*, *Astron Astrophys. Suppl. Ser.* 92, 317 (1992)
2. E J. Smith, K.-P. Wenzel, D. E Page, *Science* 257, 1503 (1992).
3. A. Balogh *et al.*, *ibid.*, p. 1515.
4. T. W. Hill, A. J. Dessler, C. K. Goertz, in *Physics of the Jovian Magnetosphere* (University Press, Lanham, MD, 1983), p. 353
5. J. F. Carbary, *Geophys. Res. Lett.* 7, 29 (1980).
6. J. A. Simpson *et al*, *Science* 188, 455 (1975).
7. S. M. Krimigis *et al.*, *ibid.* 206, 977 (1979).
8. S M. Krimigis *et al.*, *ibid.* 204, 998 (1979).
9. J. H. Trainor *et al.*, *ibid.* 183, 311 (1974).

10 We thank the project offices of Ulysses at the Euro-

pean Space Technology Center and the Jet Propulsion Laboratory and the spacecraft and mission operations teams of the European Space Association and the National Aeronautics and Space Administration for help and cooperation in carrying out this experiment. We thank M. Bruns and S. Mazuk for their work in preparing the data, G. Umlauft and K. Fischer for their work in building and calibrating the instrument, W. I. Axford and V. M. Vasyliunas for discussions and suggestions, and A. Balogh and B. Forsythe for supplying data in advance of publication. This work was supported by the Max Planck Gesellschaft, by the Deutsche Agentur für Raumfahrtangelegenheiten under grant number 50ON91050 (MPAE part). Work at Imperial College was supported by the United Kingdom Science and Engineering Research Council and at Kiruna by the Swedish National Space Board.

27 May 1992; accepted 31 July 1992

Regulation of Dynein-Driven Microtubule Sliding by the Radial Spokes in Flagella

Elizabeth F. Smith and Winfield S. Sale

The regulation of microtubule sliding in flagellar axonemes was studied with the use of *Chlamydomonas* mutants and in vitro assays. Microtubule sliding velocities were diminished in axonemes from mutant cells missing radial spoke structures but could be restored upon reconstitution with dynein from axonemes with wild-type radial spokes. These experiments demonstrate that the radial spokes activate dynein's microtubule sliding activity.

Dyneins are a family of adenosine triphosphatases that cause microtubule sliding in ciliary and flagellar axonemes (*1–3*) and directed vesicle transport along cytoplasmic microtubules (*4*). Although much is known about the structure and action of axonemal dyneins (*5*), little is known about how their activity is regulated or how active microtubule sliding is translated into principal and reverse bends. Because dynein generates force in a single direction relative to microtubule polarity (*6*), and because variation in microtubule sliding along the length of the axoneme appears to generate bends (*3, 7*), dynein-driven microtubule sliding must be regulated spatially and temporally.

Structural (*8*) and genetic (*9*) evidence implicates the radial spokes as regulatory components. The spokes are protein complexes (*10, 11*) that attach to each doublet microtubule immediately adjacent to the inner row of dynein arms and project centrally (Figs. 1 and 2A). Mutants of the biflagellate alga *Chlamydomonas* that are deficient in radial spokes either are paralyzed or have altered motility (*9, 11*). Certain suppressor mutations that bypass the requirement of normal radial spokes for motility contain defects in the dynein arms (*12, 13*). To test the hypothesis that radial spokes interact with dynein, we analyzed microtubule sliding velocities in isolated axonemes from mutant strains of *Chlamydomonas*.

In the sliding disintegration assay (*14*), flagellar axonemes are isolated, treated with protease, and exposed to adenosine triphosphate (ATP) that induces the doublet microtubules to slide apart in a telescoping fashion (*15–17*). Thus, dynein-induced doublet microtubule sliding velocities can be uncoupled from flagellar bending and quantified in both paralyzed and motile mutants (*18, 19*). Altered sliding velocities would reflect an interaction between spokes and dynein. We found that the spokeless mutant (*pf*14, which had paralyzed flagella) had sliding velocities (2.0 ± 0.9 μm/s, $n = 51$) that were significantly slower ($P < 0.001$) than those of wild type (6.1 ± 1.4 μm/s, $n = 34$) (*15*). Therefore, in the absence of the radial spokes dynein (either inner or outer arms) is apparently not as efficient in translocating the doublet microtubules.

We focused our study on the inner dynein arms because they are necessary and sufficient for motility (*18*) and have features that suggest they might be targets of regulation (*13, 19–21*). The three subtypes of inner dynein arms are located in distinct positions in the axoneme, perhaps indicating functional specialization (*20*). Several inner arm components are phosphoproteins (*21*), and defects in phosphorylation may suppress paralysis in mutants without radial spokes (*13*). The spokes are also located immediately adjacent to the inner dynein arms, perhaps providing direct structural interactions. Finally, the inner dynein arms can be structurally and functionally reconstituted in vitro (*19*), which provides a new experimental approach for the exchange of dynein arms on axonemes of distinct composition.

We compared the sliding velocities of a mutant without outer dynein arms, *pf*28 (motile flagella), with those of a mutant that lacks both radial spokes and outer dynein arms, *pf*14*pf*28 (immotile flagella) (Fig. 2). Axonemes from *pf*14*pf*28 had significantly ($P < 0.001$) slower sliding velocities (*15*) (0.5 ± 0.2 μm/s, $n = 42$) than *pf*28 axonemes (1.3 ± 0.5 μm/s, $n = 43$), indicating that the presence or absence of spokes affects the microtubule-translocating efficiency of the inner dynein arms. To determine whether dynein was activated through a modification induced by the spokes, we used an in vitro reconstitution system (*19*) to switch the inner dynein arms of *pf*28 axonemes with those of *pf*14*pf*28 axonemes.

Reconstitution experiments with inner dynein arms that had (in *pf*28) or had not (in *pf*14*pf*28) been exposed to spokes indicated that the radial spokes induced a modification of the inner dynein arms that was maintained in the subsequent absence of radial spokes (Table 1). Both *pf*28 and *pf*14*pf*28 axonemes reconstituted with their respective extracts slid at their original velocities, indicating that the extraction and reconstitution procedure did not by itself induce any changes in dynein activity. Extracted axonemes from *pf*28 reconstituted with inner arms from *pf*14*pf*28 slid at the velocity of intact *pf*28 axonemes. Furthermore, extracted axonemes from *pf*14*pf*28 reconstituted with inner arms from *pf*28 also slid at the velocity of intact *pf*28 axonemes. Therefore, the inner dynein arms from *pf*28 exposed to radial spokes remain in an activated state after extraction and reconstitution without the radial spokes.

Similar results were obtained in a potassium acetate (KCH_3COO) buffer (Table 1), which was reported to produce microtubule sliding velocities that closely parallel those calculated for beating, reactivated axonemes (*22*). Although all sliding velocities increased, their relative differences were not affected.

The increased sliding velocity of *pf*14*pf*28 axonemes reconstituted with inner

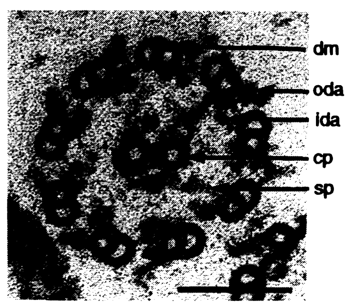

Fig. 1. Electron micrograph of axonemal cross section from wild-type *Chlamydomonas* flagella indicating the doublet microtubules (dm), outer (oda) and inner (ida) dynein arms, central pair of microtubules (cp), and radial spokes (sp). Axonemes were isolated and prepared for electron microscopy as described in (*19*). Scale bar, 100 nm.

Department of Anatomy and Cell Biology, Emory University School of Medicine, Atlanta, GA 30322.